miR-144-3p/miR-451a promotes lymphovascular invasion through repression of PTEN/p19 in rectal neuroendocrine tumors

running head; miR-144-3p/miR-451a promotes LVI in rectal neuroendocrine tumors

Noriaki Murayama,[1] Koichi Okamoto,[1] Tadahiko Nakagawa,[1] Jinsei Miyoshi,[1] Kensei Nishida,[2] Tomoyuki Kawaguchi[1], Kaizo Kagemoto,[1] Shinji Kitamura,[1] Beibei Ma,[1] Hiroshi Miyamoto,[1] Naoki Muguruma,[1] Mitsuyasu Yano,[3] Koichi Tsuneyama,[4] Takahiro Fujimori,[5] Yasushi Sato[1] and Tetsuji Takayama[1]

1) Department of Gastroenterology and Oncology, Institute of Biomedical Sciences, Tokushima University Graduate School, Tokushima, Japan.

2) Department of Pathology and Laboratory Medicine, Institute of Biomedical Sciences, Tokushima University Graduate School, Tokushima, Japan.

3) Department of Gastroenterology, Tokushima Prefectural Central Hospital, Tokushima, Japan.

4) Department of Pathology and Laboratory Medicine, Graduate School of Biomedical Sciences, Tokushima University, Tokushima, Japan.

5) Diagnostic Pathology Center, Shinko Hospital, Kobe, Japan

Address Correspondence to Tetsuji Takayama, M.D. Ph.D., 3-18-15, Kuramoto-cho, Tokushima, 770-8503, Japan. Tel: 088-633-7124. Fax: 088-633-9235. E-mail: takayama@tokushima-u.ac.jp

Disclosure statement: The authors declare that they have no conflict of interest.

Acknowledgements: The authors gratefully acknowledge helpful assistance of Hiroki Noguchi and Ryota Seki in this research. This work was supported by JSPS KAKENHI Grant Number 16K19347.

Abstract

Background and Aim: Although rectal neuroendocrine tumor (NET-G1) have potential metastatic capability, even among small tumors, no predictive biomarker for invasion and metastasis has been reported. We analyzed microRNA (miRNA) expression profiles in rectal NET-G1 tissues with and without lymphovascular invasion (LVI). Moreover, we then investigated their target genes to clarify the mechanism of invasion/metastasis in NET-G1.

Methods: miRNA array analysis was performed using 7 rectal NET-G1 tissues with LVI and 7 without LVI. miRNA expression was confirmed by quantitative real-time PCR. A NET cell line H727 was transfected with miRNA mimic or target gene small interfering RNA, and migration and invasion assays were performed.

Results: The expression levels of miR-144-3p and miR-451a were significantly higher in NET-G1 with LVI versus without LVI, as determined by miRNA array analysis and RT-qPCR. A significant correlation was observed between miR-144-3p and miR-451a expression levels, strongly suggesting miR144/451 cluster overexpression in NET-G1 with LVI. Bioinformatic analysis of target genes revealed that miR-144-3p and miR-451a directly interact with PTEN and p19 mRNA, respectively. Immunohistochemistry revealed significantly lower expression of PTEN and p19 in NET-G1 tissues with LVI than in those without LVI. The miR-144-3p and miR-451a mimic significantly increased cell migration/invasion capability, respectively. Knockdown of PTEN and p19 induced significant augmentation of cell invasion and migration capability, respectively.

Conclusions: Our data suggest that overexpression of miR-144/miR-451 cluster promotes LVI via repression of PTEN and p19 in rectal NET-G1 cells. miR-144/451 cluster may be a novel biomarker for predicting invasion/metastasis in rectal NET-G1.

Keywords: rectal NET-G1, lymphovascular invasion, miR-144-3p/451a, PTEN, p19

Introduction

Although rectal neuroendocrine tumors (NET)-G1, previously referred to as carcinoid tumors, are relatively rare among patients with digestive tract diseases, they account for 9% to 55% of gastrointestinal NET[1-3]. Recently, rectal NET-G1 has often been found during colonoscopy, probably due to the increased use of screening colonoscopy and advancement of imaging technologies[4]. Previous studies reported that the metastatic potential of rectal NET-G1 is dependent on the tumor size and depth of invasion[5, 6] and, therefore, a therapeutic strategy for rectal NET-G1 has been devised; i.e., a small rectal NET-G1 less than 10 mm in size with limited invasion to the submucosal layer is conventionally treated by local resection, including endoscopic resection, because the metastatic capability of such a lesion is very low[2, 7]. However, it has been reported that a small rectal NET-G1 less than 10 mm in size also has potentially metastatic capability[8, 9]. Therefore, it is difficult to diagnose metastasis based on the size and invasion depth of tumors. As a result, it is necessary to clarify the mechanism of metastasis in rectal NET-G1 and to find a new biomarker for metastasis.

MicroRNAs (miRNAs) are a class of small noncoding RNAs that widely regulate gene expression and play an important role in various biological processes[10, 11]. Several studies have reported that miRNAs are closely associated with invasion and metastasis in various cancers[12-14]. Only 2 studies have investigated miRNA profiles in colorectal NET tissues. Wang and colleagues performed miRNA microarray analysis on NET-G1 and neuroendocrine carcinoma (NEC) tissues, and compared the miRNA profiles with those of non-neoplastic disease and normal mucosa[15, 16]. However, they did not investigate the relevance of miRNA in invasion and metastasis of NETs. Mitsuhashi and associates reported that positive status for miR885-5p and CpG island methylator phenotype (CIMP) may be useful as biomarkers for predicting biological malignancy in small rectal NETs[17]. However, they did not examine target genes of miR885-5p and, therefore, the underlying mechanism

by which miRNA885-5p induces malignant potential is unknown. In the present study, we first compared miRNA expression profiles in rectal NET-G1 with and without lymphovascular invasion (LVI) to identify putative miRNAs involved in LVI and metastasis of rectal NET-G1. We then searched their target genes and investigated the underlying mechanism by which miRNA causes invasion and metastasis of NET cells.

Methods

Patients and tissue samples

This study was approved by the ethics committee of Tokushima University Hospital (Tokushima, Japan). We collected formalin-fixed paraffin-embedded (FFPE) tissues from 33 cases of rectal NET-G1 removed by endoscopic resection from January 2012 through March 2017. Written informed consent was obtained from all patients. The histological diagnosis of rectal NET-G1 was made independently by 2 pathologists (TF and KT) according to World Health Organization (WHO) 2019 criteria[18]. Among 33 cases of rectal NET-G1, we selected 7 patients who had rectal NET-G1 tumors with LVI and 7 patients who had rectal NET-G1 tumors without LVI for miRNA array analysis. Patient baseline characteristics are shown in Table 1. Chromogranin A and synaptophysin staining were performed to detect NET tumor cells. Tumor cell proliferation activity was evaluated using the Ki-67 labeling index. D2-40 and Victoria blue staining were performed to evaluate LVI.

Cell line

Since no primary human gastrointestinal NET-G1 cell line is commercially available, a human bronchial NET-G1 cell line (H727) obtained from the American Type Culture Collection (Manassas, VA) was used. Cells were cultured in RPMI1640 medium containing 10% fetal bovine serum.

MiRNA microarray

Total RNA was extracted using a miRNeasy FFPE Kit (Qiagen, Hilden, Germany) after macrodissection of 16-μm thick rectal NET-G1 tissue slices. A miRNA microarray was performed using SurePrint human miRNA Microarrays rel.21 (Agilent Technologies, Palo Alto, CA), as previously described[19]. Raw intensity miRNA data were analyzed by GeneSpring GX12 (Agilent Technologies). The candidate miRNAs were selected under the following conditions: miRNAs with fluorescence intensity of 15 or more, a fold change of 2 or more, and a p-value of less than 0.05 for 4 or more of the 7 specimens.

Quantitative realtime-PCR (qRT-PCR)

Levels of mature miRNA and mRNA were measured employing TaqMan qRT-PCR. The primers and probes used are described in Supplementary Table 1. The relative expression level of each gene was expressed according to the 2-ΔΔ cycle threshold (Ct) method.

Target gene and pathway analyses

Ingenuity Pathway Analysis (IPA) (http://www.ingenuity.com), miRDB (http://www.mirdb.org), and TargetScan (http://www.targetscan.org/) were used to predict the target genes of miRNAs. Functional pathways related to the differentially expressed genes were assessed by IPA.

Overexpression and knockdown experiments

H727 cells were transfected with miR-144-3p mimic or miR-451a mimic (mirVana miRNA mimic®, Life Technologies, Karlsruhe, Germany) to overexpress each miRNA using Lipofectamine RNAiMAX (Invitrogen, Carlsbad, CA), as described previously[19]. Similarly,

H727 cells were transfected with small interfering RNA (siRNA) targeting PTEN (Cell Signaling Technology, Inc.) or CDKN2D/p19 gene (Silencer Select s2851, Ambion, Austin, TX) to knockdown each gene, as described previously[19].

Details of cell invasion assay, wound healing assay, immunohistochemistry and statistics are provided in Supplementary information.

Results

Comparison of miRNA expression profile between rectal NET-G1 with and without LVI

To explore miRNAs that are closely associated with LVI, we first performed miRNA microarray analysis and compared the miRNA expression profiles between 7 rectal NET-G1 tissues with LVI and 7 tissues without LVI. Baseline characteristics of the patients with NET-G1 with and without LVI are summarized in Table 1. No significant differences in gender, age, and tumor size were observed between the 2 groups. The miRNAs in the LVI (+) group that were significantly higher or lower than those in the LVI (-) group, are listed in Supplementary Table 2. Of these 8 miRNAs, we selected the 5 miRNAs with the highest fold change; i.e., miR-144-3p, miR-451a, miR-486, miR-551b-3p, and miR-10b-5p. The average fold changes of these miRNAs were 52.13, 10.56, 3.99, 2.82, and 2.29 respectively.

Validation of miRNA expression by qRT-PCR

To validate the differential expression of the 5 miRNAs in rectal NET-G1 tissues, we performed qRT-PCR using an additional 5 rectal NET-G1 tissues with LVI and 5 NET-G1 tissues without LVI. The levels of miR-144-3p and miR-451a in rectal NET-G1 tissues with LVI were significantly higher than in those without LVI (respectively $p<0.05$; Fig.1a,b). The levels of miR-486 and miR-10b in NET-G1 with LVI (+) were higher than in those with LVI (-),

but did not reach a statistically significant difference (p=0.08 and p=0.08 respectively; Fig.1c,e). In contrast, the levels of miR-551b-3p in NET-G1 with LVI (+) was similar to those in LVI (-) (p=0.40; Fig. 1d). Therefore, we selected miR-144-3p and miR-451a as putative miRNAs involved in the invasion/metastasis of rectal NET-G1 in the following experiments.

Since miR-144-3p and miR-451 are reported to be up-regulated as a miR144/451 cluster in insulinoma[20], we examined the correlation of expression levels between miR-144-3p and miR-451a. A significant correlation was observed between miR-144-3p and miR-451a levels (Fig.1f; p<0.01), indicating their up-regulation as a miR144/451 cluster gene in NET-G1 cells.

In addition, although miR-144-5p, miR-4732-3p, and miR-4732-5p were reportedly related to the miR144/451 cluster[21], there was no significant increase in their expression levels of the microarray data (Supplementary Table 3).

Putative target genes of miR-144-3p and miR-451a

To search for putative target genes of miR-144-3p and miR-451a, we first performed Ingenuity Pathway Analysis (IPA) using the keywords “MIR144” or “MIR451”, and found the respective candidate target genes; CD34, CELF2, PTEN, and VCAN for miR-144-3p and p19 (CDKN2D) and CELF2 for miR-451a. The IPA networks, which associated with “Invasion of cells” and “Cell cycle progression” for these genes, are shown in Supplementary Figure 1. PTEN and CELF2 were identified by miRDB and TargetScan analysis as genes that are directly bound to miR-144-3p. However, the score of PTEN was much higher than that of CELF2, suggesting PTEN as a much better target for miR-144-3p. In fact, the 2917 to 2923 sequence in the 3'- untranslated region (UTR) of the PTEN gene completely matched the ACAGUAU sequence of miR-144-3p (Fig.2). On the other hand, only p19 was identified as a gene which directly binds to miR-451a. The 240 to 246 sequence in the 3'-UTR of p19

completely matched the AACCGUU sequence of miR-451a. Thus, these genes were postulated to be the most likely candidate targets of the miRNAs.

Decreased expression of PTEN and p19 in rectal NET-G1 with LVI

To examine the protein expression of the 2 target genes, we performed immunohistochemical staining for PTEN and p19 using 5 rectal NET-G1 with LVI and 5 rectal NET-G1 without LVI. Representative staining patterns are shown in Figure 3. PTEN was strongly stained in the nucleus as well as the cytosol of NET-G1 cells without LVI, but showed almost no staining in NET-G1 cells with LVI (Fig.3a). Quantitative analysis of staining for PTEN, showed that the immunohistochemical score in the LVI(+) group was significantly lower than in the LVI(-) group (1.1±0.9 vs 8.5±2.0; $p<0.01$; Fig.3b). Similarly, p19 showed obvious staining in the cytoplasm of NET-G1 cells without LVI, but was very faintly stained in NET-G1 cells with LVI (Fig.3c). Quantitative analysis of staining for p19 showed that the score in LVI(+) group was significantly lower than in the LVI(-) group (2.4±0.5 vs 7.2±4.5, $p<0.05$; Fig.3d). These results suggest that miR-144-3p and miR-451a inhibited PTEN and p19 expression, respectively, through repression of those mRNAs in rectal NET-G1 with LVI.

Decreased levels of PTEN and p19 mRNAs in an H727 NET cell line transfected with miR-144-3p mimic or miR-451a mimic

To further confirm the interaction of miR-144-3p with PTEN and interaction of miR-451a with p19, respectively, we performed transfection experiments using an H727 NET cell line. Because both miR-144-3p and miR-451a expression levels in H727 cells were very low as revealed by qRT-PCR (Supplementary Table 4), we transfected miR-144-3p or miR-451a mimics into H727 cells and evaluated mRNA expression levels of PTEN and p19 with qRT-

PCR. Sufficient expression of miR-144-3p in H727 cells transfected with miR-144-3p mimic was confirmed by qRT-PCR (data not shown). Levels of PTEN mRNA expression in H727 cells transfected with miR-144-3p mimic were significantly decreased to 32 ± 6 % of those in control cells ($p<0.01$; Fig.4a). Similarly, sufficient expression of miR-451a in H727 cells transfected with miR-451a mimic was confirmed by qRT-PCR (data not shown). The levels of p19 mRNA in H727 cells transfected with miR-451a mimic were significantly decreased to 46 ± 7 % of those in control cells ($p<0.01$; Fig.4b). Thus, we confirmed that miR-144-3p and miR-451a inhibited transcription of their respective target genes in H727 cells.

Effect of miRNA mimics on cell migration and invasion capability

To prove that miR-144-3p and miR-451a are closely associated with the migration/invasion capability of rectal NET-G1, we assessed cell migration/invasion capability using H727 cells transfected with miR-144-3p or miR-451a mimic. Representative images of the wound healing assay are shown in Figure 4c. The migration distance of H727 cells transfected with miR-144-3p or miR-451a mimic was significantly greater than that of control cells ($p<0.05$ respectively). Quantitative analysis revealed that the migration distance of H727 cells transfected with miR-144-3p or miR-451a mimic (0.54±0.13 or 0.85±0.11) was significantly greater than that of control cells (0.27±0.12, $p<0.05$ respectively; Fig.4d). In the invasion assay analysis, the fluorescence intensity of invading cells in H727 cells transfected with miR-144-3p ($13.5x10^5 \pm 1.8x10^5$) or miR-451a mimic ($14.9x10^5 \pm 3.1x10^5$) was significantly higher than that in control cells ($10.5x10^5 \pm 0.5x10^5$; $p<0.05$ respectively; Fig.4e). These results suggest that miR-144-3p and miR-451a enhanced the migration and invasion capability in NET cells.

Knockdown of PTEN and p19 genes enhanced cell migration and invasion capability

We then knocked down the PTEN or p19 gene in H727 cells and investigated the change in cell migration and invasion capability. The relative levels of PTEN and P19 mRNA in H727cells transfected with siRNA were reduced to 2.9 ± 1.8% and 10.2 ± 3.6%, respectively, of that in control cells (Fig.5a,b). Representative images of the wound healing assay are shown in Figure 5c. The migration distance in H727 cells transfected with PTEN siRNA or p19 siRNA was significantly greater than that in control cells. Quantitative analysis revealed that the migration distance for H727 cells transfected with PTEN siRNA (0.82 ± 0.10) or p19 siRNA (0.82 ± 0.07) was significantly higher than that of control cells (0.61 ± 0.11; $p<0.05$ respectively; Fig.5d). In the invasion assay analysis, the fluorescence intensity of invading cells in H727 cells transfected with PTEN siRNA ($13.3x10^5 \pm 0.9x10^5$) or p19 siRNA ($14.0x10^5 \pm 1.0x10^5$) was significantly higher than that in control cells ($11.8x10^5 \pm 1.3x10^5$; $p<0.05$ respectively; Fig.5e). These results suggest that miR-144-3p and miR-451a enhanced migration and invasion capability probably through repression of PTEN and p19, respectively, in NET cells.

Discussion

In this study, we found overexpression of miR-144-3p and miR-451a as a miRNA144/451 cluster in rectal NET-G1 tissues with LVI, as demonstrated using miRNA microarray analysis and qRT-PCR. We also revealed that miR-144-3p and miR-451a inhibited mRNA transcription of PTEN and p19, respectively, as target genes. Additionally, we demonstrated that overexpression of miR-144-3p and miR-451a significantly enhanced cell migration/ invasion capability in NET cells. Conversely, knockdown of PTEN or p19 gene in NET cells significantly augmented cell migration/invasion capability. Thus, our data suggest that miR-144-3p and miR-451a (miRNA144/451 cluster) caused LVI in rectal NET-G1 cells probably through repression of PTEN and p19, leading to subsequent metastasis and poor prognosis.

This is the first report showing that miR-144/451 cluster plays a pivotal role possibly via inhibition of PTEN and p19 in LVI of rectal NET-G1.

It has been reported that miR-144-3p is upregulated in several kinds of cancers including thyroid and breast cancers, and is closely associated with malignant progression (i.e., invasion and metastasis) and poor prognosis[22, 23]. Similarly, miR-451a was reportedly upregulated in several types of cancers including gastric, prostate, and esophageal cancers, in association with a poor prognosis[24, 25]. Our finding that miR-144-3p and miR-451 were overexpressed in rectal NET-G1 with LVI is consistent with those previous reports. Namely, miR-144-3p and miR-451a serve as oncogenic miRNAs associated with invasion and metastasis, possibly leading to a poor prognosis in rectal NET-G1.

It is noteworthy that miR144-3p and miR-451a were up-regulated as an miRNA cluster in NET-G1 cells. miR-144-3p and miR-451a were reported to be located on chromosome 17 at 17q11.2, only 100 bp away from each other[26]. In general, miRNA cluster is reportedly more stable and reliable than individual miRNAs to serve as an oncogenic miRNA or oncosupressive miRNA[21, 27]. Recently, it has been reported that miR144 and miR451 (miR144/451) are transcribed as one pri-microRNA during erythropoiesis[28]. It has also been reported that miR144/451 expression is repressed by transcription factor RUNX1, whereas the cluster transcription is positively regulated by transcription factors GATA1 and TAL1 in hematopoietic cells[29]. Although the mechanism by which miR144/451 expression is regulated in NET cells is currently unknown, it is possible that these transcription factors may affect expression of the cluster in rectal NET cells.

There has been only a single study showing that miR-144-3p and miR-451a are up-regulated as a cluster in tumors; Jiang and associates reported that miR144/451 cluster was up-regulated in insulinoma compared with normal islet cells, suggesting the importance of the miR144/451 cluster in the development of insulinoma[20]. We found overexpression of

miR144/451 cluster in NET-G1 tissues. Interestingly, Wu and associates reported that 9 miRNAs were significantly upregulated in bromocriptine-resistant prolactinoma compared with bromocriptine-sensitive prolactinoma[30]; miR-144 and miR-451a were included in those miRNAs. In this context, it is plausible that miR-144/451 cluster may play an important role as oncogenic miRNAs in the development and malignant progression of endocrine tumors such as insulinoma, prolactinoma, and NET-G1 cells.

There have been some contradictory studies on miR-144 or miR-451a in colorectal cancers. Iwaya and associates reported that downregulation of miR-144 leads to a poor prognosis in colorectal cancer patients via activation of the mTOR signaling pathway[31]. Ruhl and associates reported that miR-451a inhibited colorectal cancer proliferation[32]. Moreover, Gao and associates reported that silenced expression of miR-144/451 cluster is closely associated with cell migration, invasion, and proliferation in esophageal cancer. These findings suggest that miR-144-3p and miR-451a promote invasion and metastasis in NET-G1 cells but may inhibit progression of colorectal cancer cells and esophageal cancer cells. That is, miR-144-3p and miR-451a may serve as an oncogenic miRNA or oncosuppressor miRNA in a cancer tissue-specific manner.

We bioinformatically identified PTEN as a target gene of miR-144-3p, and revealed their close association in a NET cell line. PTEN is a tumor suppressor protein that negatively regulates phosphatidylinositol 3-kinase (PI3K), and consequently AKT/mTOR pathway. PTEN is also reportedly involved in regulation of cell apoptosis, cell cycle entry, cell proliferation, and cell adhesion. PTEN is ubiquitously expressed in humans, and its inactivation is associated with carcinogenesis and cancer progression[33]. In fact, previous studies have reported that low expression of PTEN is closely related with tumor progression and aggressive biological behavior in NETs[34, 35]. Although in those studies, miRNAs were not examined in the tumors, miR-144-3p might be overexpressed, thereby possibly inhibiting

PTEN expression. Importantly, it is now well recognized that PI3K/AKT/mTOR pathway is activated in advanced gastrointestinal and pancreatic NETs. Therefore, the mTOR specific inhibitor everolimus was found to be effective on those NETs in clinical studies and is currently recommended as first-line treatment for NETs[36]. This fact is quite compatible with our finding that the miR144-PTEN axis activates PI3K/AKT/mTOR pathway in potentially malignant rectal NETs.

We also identified p19, a member of the Inhibitor of CDK4 (INK4) family, as a target of miR-451a. Downregulation of p19 is reported to promote cancer development in several kinds of cancers including testicular cancer[37] and osteosarcoma[38]. Our finding that miR-451a inhibited p19 mRNA expression, thereby serving as an oncogenic miRNA, is consistent with a previous study[20]. Thus, our data indicated that miR-144-3p and miR-451a were overexpressed as a cluster, and resultant down-regulation of PTEN and p19 cooperatively promoted migration/invasion capability in rectal NET-G1 cells. Importantly, the tumor size examined in this study was smaller than 10 mm, but the malignant or benign features of NET-G1 may be distinguishable by applying liquid biopsy with miR-144/451 cluster (miR-144-3p and miR-451a).

There were 3 limitations in this study. First, only a small number of NET-G1 tissues were examined for miRNA expression. The partial discrepancy between the microarray and qRT-PCR data may be partly explained by the small sample size as well as different samples used. Although rectal NET-G1 is not a common disease, the data obtained in this study should be confirmed in a greater number of cases in the future. Second, we used NET-G1 tissues with and without LVI to compare miRNA expression, but did not use metastatic and non-metastatic lymph node tissues. Because of the low prevalence of lymph node metastasis (0%-5.5%) in rectal NET-G1[2, 8], it was difficult to obtain those tissues. Third, due to the lack of commercial availability, we could not use a primary human

gastrointestinal NET-G1 cell line and instead used a human bronchial NET-G1 cell line. Our results should be confirmed using a rectal NET-G1 cell line if one is established in the future.

In conclusion, our study demonstrated that miR-144-3p and miR-451a were upregulated as a cluster in rectal NET-G1 cells. The miR144-3p and miR-451a expression was strongly associated with migration/invasion capability in rectal NET-G1 through repression of PTEN and p19. Thus, liquid biopsy of the miR-144-3p and miR-451a may be a novel biomarker for predicting metastasis in patients with rectal NET-G1.

References

1 Modlin IM, Sandor A. An analysis of 8305 cases of carcinoid tumors. *Cancer*. 1997; **79**: 813-29.
2 Jetmore AB, Ray JE, Gathright JB, Jr., McMullen KM, Hicks TC, Timmcke AE. Rectal carcinoids: the most frequent carcinoid tumor. *Dis Colon Rectum*. 1992; **35**: 717-25.
3 Olney JR, Urdaneta LF, Al-Jurf AS, Jochimsen PR, Shirazi SS. Carcinoid tumors of the gastrointestinal tract. *Am Surg*. 1985; **51**: 37-41.
4 Scherubl H. Rectal carcinoids are on the rise: early detection by screening endoscopy. *Endoscopy*. 2009; **41**: 162-5.
5 Anthony LB, Strosberg JR, Klimstra DS*, et al.* The NANETS consensus guidelines for the diagnosis and management of gastrointestinal neuroendocrine tumors (nets): well-differentiated nets of the distal colon and rectum. *Pancreas*. 2010; **39**: 767-74.
6 Ramage JK, De Herder WW, Delle Fave G*, et al.* ENETS Consensus Guidelines Update for Colorectal Neuroendocrine Neoplasms. *Neuroendocrinology*. 2016; **103**: 139-43.
7 Koura AN, Giacco GG, Curley SA, Skibber JM, Feig BW, Ellis LM. Carcinoid tumors of the rectum: effect of size, histopathology, and surgical treatment on metastasis free survival. *Cancer*. 1997; **79**: 1294-8.
8 Soga J. Carcinoids of the rectum: an evaluation of 1271 reported cases. *Surg Today*. 1997; **27**: 112-9.
9 Shinohara T, Hotta K, Oyama T. Rectal carcinoid tumor, 6 mm in diameter, with lymph node metastases. *Endoscopy*. 2008; **40 Suppl 2**: E40-1.
10 Lee RC, Ambros V. An extensive class of small RNAs in Caenorhabditis elegans. *Science*. 2001; **294**: 862-4.
11 Guo H, Ingolia NT, Weissman JS, Bartel DP. Mammalian microRNAs predominantly act to decrease target mRNA levels. *Nature*. 2010; **466**: 835-40.
12 Calin GA, Croce CM. MicroRNA signatures in human cancers. *Nat Rev Cancer*. 2006; **6**: 857-66.
13 Croce CM. Causes and consequences of microRNA dysregulation in cancer. *Nat Rev Genet*. 2009; **10**: 704-14.
14 Malczewska A, Kidd M, Matar S, Kos-Kudla B, Modlin IM. A Comprehensive Assessment of the Role of miRNAs as Biomarkers in Gastroenteropancreatic Neuroendocrine Tumors. *Neuroendocrinology*. 2018; **107**: 73-90.
15 Wang M, Xia X, Chu W*, et al.* Roles of miR-186 and PTTG1 in colorectal neuroendocrine tumors. *Int J Clin Exp Med*. 2015; **8**: 22149-57.
16 Hamfjord J, Stangeland AM, Hughes T*, et al.* Differential expression of miRNAs in colorectal cancer: comparison of paired tumor tissue and adjacent normal mucosa using high-throughput sequencing. *PLoS One*. 2012; **7**: e34150.
17 Mitsuhashi K, Yamamoto I, Kurihara H*, et al.* Analysis of the molecular features of rectal carcinoid tumors to identify new biomarkers that predict biological malignancy. *Oncotarget*. 2015; **6**: 22114-25.
18 Rindi G, Komminoth P, Scoazec J, Shia J. Colorectal neuroendocrine neoplasms. *Digestive system tumors WHO classification of tumors*. 5th ed. Lyon, France: International Agency for Research on Cancer, 2019; 188-91.
19 Fujino Y, Takeishi S, Nishida K*, et al.* Downregulation of microRNA-100/microRNA-125b is associated with lymph node metastasis in early colorectal cancer with submucosal invasion. *Cancer Sci*. 2017; **108**: 390-7.
20 Jiang X, Shan A, Su Y*, et al.* miR-144/451 Promote Cell Proliferation via Targeting PTEN/AKT Pathway in Insulinomas. *Endocrinology*. 2015; **156**: 2429-39.
21 Gao Z, Zhang P, Xie M, Gao H, Yin L, Liu R. miR-144/451 cluster plays an oncogenic role in esophageal cancer by inhibiting cell invasion. *Cancer Cell Int*. 2018; **18**: 184.
22 Cao HL, Gu MQ, Sun Z, Chen ZJ. miR-144-3p Contributes to the Development of Thyroid Tumors Through the PTEN/PI3K/AKT Pathway. *Cancer Manag Res*. 2020; **12**: 9845-55.
23 Yu L, Yang Y, Hou J*, et al.* MicroRNA-144 affects radiotherapy sensitivity by promoting proliferation, migration and invasion of breast cancer cells. *Oncol Rep*. 2015; **34**: 1845-52.
24 Godlewski J, Nowicki MO, Bronisz A*, et al.* MicroRNA-451 regulates LKB1/AMPK signaling and allows adaptation to metabolic stress in glioma cells. *Mol Cell*. 2010; **37**: 620-32.

25 Brenner B, Hoshen MB, Purim O*, et al.* MicroRNAs as a potential prognostic factor in gastric cancer. *World J Gastroenterol*. 2011; **17**: 3976-85.
26 Pan X, Wang R, Wang ZX. The potential role of miR-451 in cancer diagnosis, prognosis, and therapy. *Mol Cancer Ther*. 2013; **12**: 1153-62.
27 Hayashita Y, Osada H, Tatematsu Y*, et al.* A polycistronic microRNA cluster, miR-17-92, is overexpressed in human lung cancers and enhances cell proliferation. *Cancer Res*. 2005; **65**: 9628-32.
28 Kretov DA, Walawalkar IA, Mora-Martin A, *et al*. Ago2-Dependent Processing Allows miR-451 to Evade the Global MicroRNA Turnover Elicited during Erythropoiesis. *Mol Cell*. 2020; **78**: 317-28 e6.
29 Kohrs N, Kolodziej S, Kuvardina ON*, et al.* MiR144/451 Expression Is Repressed by RUNX1 During Megakaryopoiesis and Disturbed by RUNX1/ETO. *PLoS Genet*. 2016; **12**: e1005946.
30 Wu ZB, Li WQ, Lin SJ*, et al.* MicroRNA expression profile of bromocriptine-resistant prolactinomas. *Mol Cell Endocrinol*. 2014; **395**: 10-8.
31 Iwaya T, Yokobori T, Nishida N*, et al.* Downregulation of miR-144 is associated with colorectal cancer progression via activation of mTOR signaling pathway. *Carcinogenesis*. 2012; **33**: 2391-7.
32 Ruhl R, Rana S, Kelley K*, et al.* microRNA-451a regulates colorectal cancer proliferation in response to radiation. *BMC Cancer*. 2018; **18**: 517.
33 Salmena L, Carracedo A, Pandolfi PP. Tenets of PTEN tumor suppression. *Cell*. 2008; **133**: 403-14.
34 Pitt SC, Davis R, Kunnimalaiyaan M, Chen H. AKT and PTEN expression in human gastrointestinal carcinoid tumors. *Am J Transl Res*. 2009; **1**: 291-9.
35 Missiaglia E, Dalai I, Barbi S*, et al.* Pancreatic endocrine tumors: expression profiling evidences a role for AKT-mTOR pathway. *J Clin Oncol*. 2010; **28**: 245-55.
36 Yao JC, Shah MH, Ito T*, et al.* Everolimus for advanced pancreatic neuroendocrine tumors. *N Engl J Med*. 2011; **364**: 514-23.
37 Bartkova J, Thullberg M, Rajpert-De Meyts E, Skakkebaek NE, Bartek J. Lack of p19INK4d in human testicular germ-cell tumours contrasts with high expression during normal spermatogenesis. *Oncogene*. 2000; **19**: 4146-50.
38 Miller CW, Yeon C, Aslo A, Mendoza S, Aytac U, Koeffler HP. The p19INK4D cyclin dependent kinase inhibitor gene is altered in osteosarcoma. *Oncogene*. 1997; **15**: 231-5.

Figure legends

Figure 1

Relative expression levels of 5 miRNAs in rectal neuroendocrine tumor (NET)-G1 tumors with and without LVI. Total RNAs were extracted from formalin-fixed paraffin-embedded (FFPE) sections of NET-G1 tumor LVI (+) (n=5) and tumor LVI(-) (n=5), and expression levels of miRNAs were determined by Taqman quantitative reverse transcription-polymerase chain reaction (RT-qPCR). (a) miR-144-3p, (b) miR-451a, (c) miR-486, (d) miR-551b-3p and (e) miR-10b. Each miRNA expression level was normalized to U6. (f) The correlation coefficient between miR-144-3p and miR-451a was 0.9879, and the p value was <0.0001. miRNA, microRNA; LVI, lymphovascular invasion; P value was analyzed using Mann–Whitney U test.

Figure 2

Predicted consequential pairing of miR-144-3p and the target regions of phosphatase and tensin homolog (PTEN), and miR-451a and the target regions of p19. TargetScan was performed to predict the target of miR-144-3p and miR-451a. The UAUGACA sequence in miR-144-3p completely matched the 3'-untranslated region of the PTEN gene. Similarly, the UUGCCAA sequence in miR-451a completely matched the 3'-untranslated region of the p19 gene.

Figure 3

Immunohistochemical staining for PTEN and p19 in rectal neuroendocrine tumor (NET-G1) with and without LVI. Representative staining patterns by labelled streptavidin-biotin (LSAB) of PTEN (a) and p19 (c) are shown. Original magnification; ×200. Immunohistochemical score for PTEN (b) and p19 (d). The immunohistochemical score was calculated by multiplication of the positive cells proportion score (0-4) and staining intensity score (0-3), as

described in Supplementary information. PTEN, phosphatase and tensin homolog; LVI, lymphovascular invasion. *p<0.05 by Mann–Whitney U test.

Figure 4

Effect of miRNA mimics on cell migration and invasion capability. H727 cells (1.5×10^6) in 6-well plates were transfected with miR-144-3p or miR-451a mimic as well as miRNA mimic-NC at a final concentration of 30 nM using the Lipofectamine RNAiMAX. (a) Levels of PTEN mRNA in H727 cells transfected with miR-144-3p mimic or mimic-NC were determined by Taqman real-time PCR. (b) Levels of p19 mRNA in H727 cells transfected with miR-451a mimic or mimic-NC were determined by Taqman real-time PCR. All experiments were performed in sextuplicate. H727 cells were transfected with miR-144-3p mimic, miR-451a mimic, or mimic-NC, and wound healing assay and invasion assay were performed. (c) Representative images of the wound healing assay after 96 h are shown. (d) Migration distance was measured at 5 points per sample~~s~~ and expressed as a mean ± standard deviation (SD) of triplicates. (e) The in vitro invasion assay was carried out using a CultreCoat 96-well Boyden Chamber Assay Kit. The fluorescence intensity for each group was measured and expressed as mean ±SD of triplicates. PTEN, phosphatase and tensin homolog; mRNA, messenger RNA; NC, negative control. *p<0.05 by Student's t test. **p<0.05 by Dunnett's test.

Figure 5

Cell migration and invasion capability of H727 cells with knock down of the PTEN or p19 gene. (a, b) PTEN or p19 gene was knocked down in H727 cells using siRNA, and wound healing and invasion assays were subsequently performed. (c) Representative images of the wound healing assay after 96 h are shown. (d) Migration distance was measured at 5 points

per sample~~s~~ and expressed as a mean ± standard deviation (SD) of triplicates. (e) The in vitro invasion assay was carried out using a CultreCoat 96-well Boyden Chamber Assay Kit. The fluorescence intensity for each group was measured and expressed as the mean ±SD of triplicates. PTEN phosphatase and tensin homolog, siRNA small interfering RNA. *p<0.05 by Mann–Whitney U test. **p<0.05 by Dunnett's test.

Supporting information

Supprementary Figure 1

Functional network analysis of miR-144-3p and miR-451a and target genes by Ingenuity Pathway Analysis (IPA). The network analysis of miR-144-3p and miR451a and their putative target genes which associated with "Invasion of cells" and "Cell cycle progression" was performed. Among the 4 putative target genes for miR-144-3p (CD34, VCAN, PTEN and CELF2), VCAN, PTEN and CELF2 were associated with these functions. Both the 2 putative target genes (CELF2 and p19 (CDKN2D)) for miR-451a were associated wih these functions.

Table 1: Baseline characteristics of the patients with rectal NET-G1

	Case	Gender	Age(y)	Tumor size	ly	v
LVI (+)	1	M	74	9 mm	-	+
	2	M	46	6 mm	+	+
	3	M	50	6 mm	+	+
	4	M	59	6 mm	+	+
	5	M	51	5 mm	-	+
	6	F	45	8 mm	+	-
	7	M	72	5 mm	+	-
LVI (-)	8	F	46	7 mm	-	-
	9	F	51	7 mm	-	-
	10	M	62	7 mm	-	-
	11	F	56	6 mm	-	-
	12	M	35	7 mm	-	-
	13	M	54	7 mm	-	-
	14	F	55	6 mm	-	-

Ly lymphatic vessel invasion, v vein invasion, LVI lymphovascular invasion

Figure1

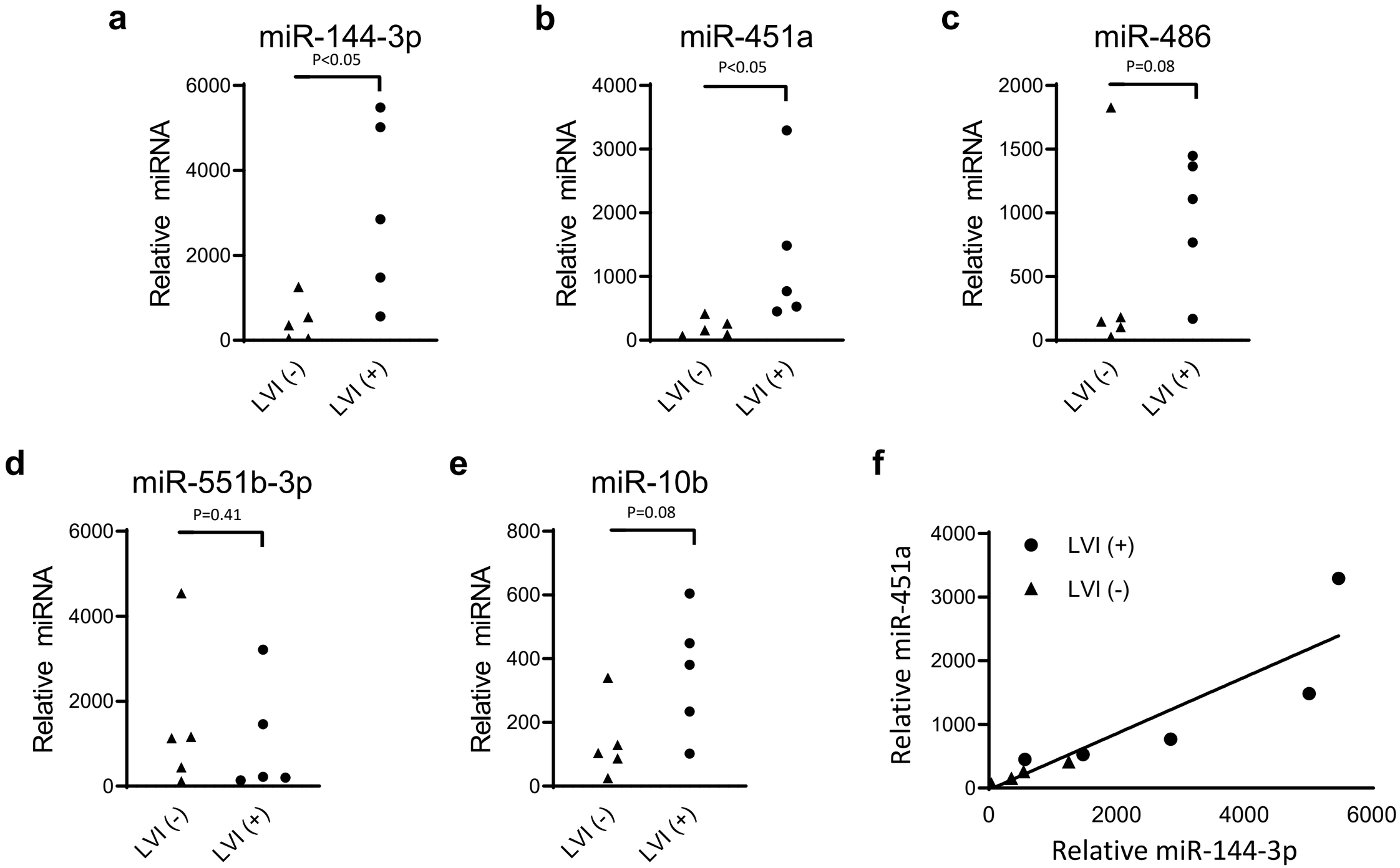
a
miR-144-3p
P<0.05
Relative miRNA
6000
4000
2000
0
LVI (-)
LVI (+)
b
miR-451a
P<0.05
Relative miRNA
4000
3000
2000
1000
0
LVI (-)
LVI (+)
c
miR-486
P=0.08
Relative miRNA
2000
1500
1000
500
0
LVI (-)
LVI (+)
d
miR-551b-3p
P=0.41
Relative miRNA
6000
4000
2000
0
LVI (-)
LVI (+)
e
miR-10b
P=0.08
Relative miRNA
800
600
400
200
0
LVI (-)
LVI (+)
f
LVI (+)
LVI (-)
Relative miR-451a
4000
3000
2000
1000
0
0
2000
4000
6000
Relative miR-144-3p

Figure2

	Predicted consequential pairing of target region (upper) and miRNA (lower)
Position 2917-2923 of PTEN 3' UTR miR-144-3p	5' ...CUCGUUUACCUUUAAAUACUGUU… 3' | | | | | | | 3' - UCAUGUAGUAGAUAUGACAU - 5'
Position 240-246 of CDKN2D (p19) 3' UTR miR-451a	5' ...GGCCACAGCCACCUAAACGGUUC… 3' | | | | | | | 3' – UUGAGUCAUUACCAUUGCCAAA - 5'

Figure3

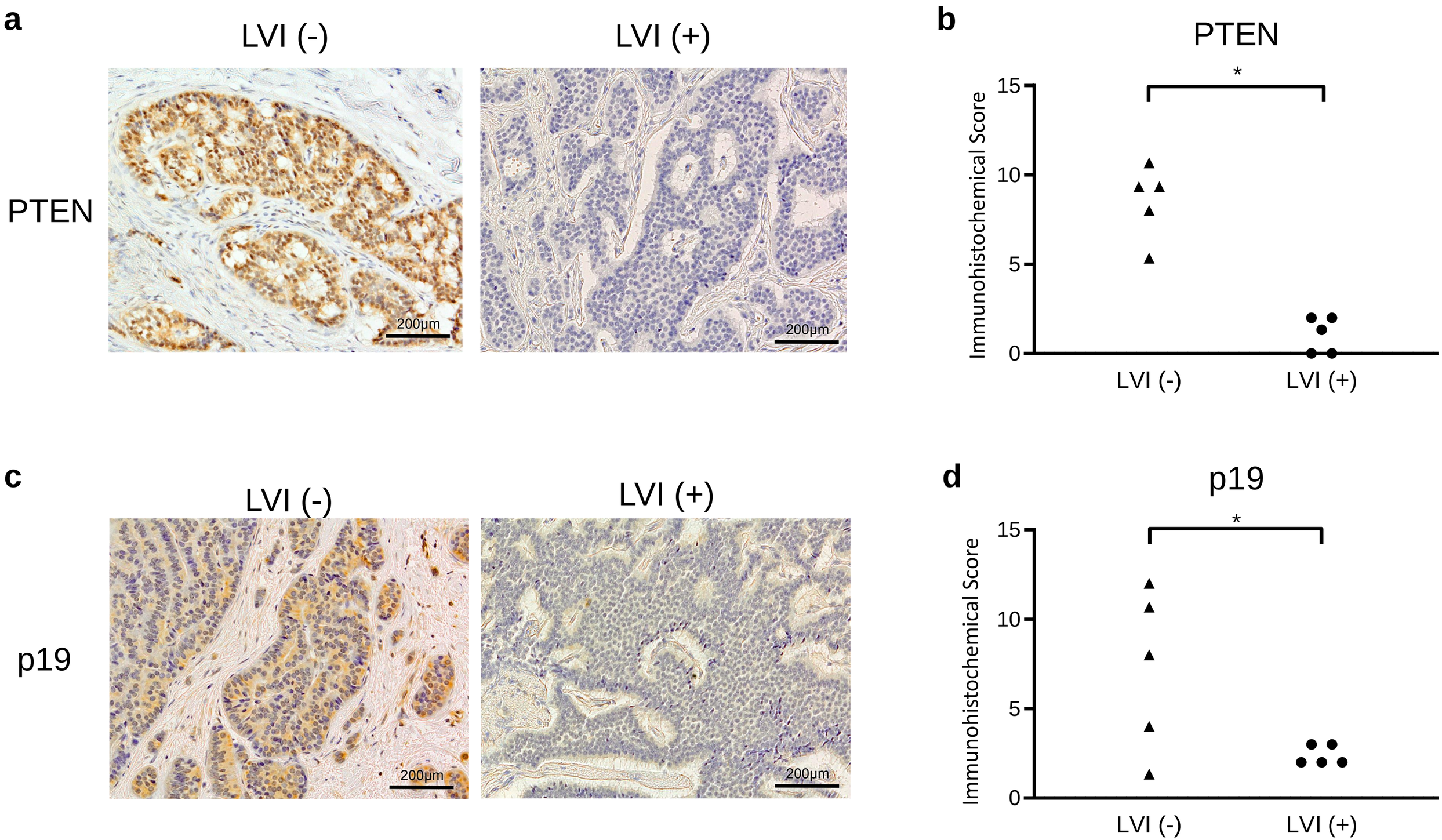
a
LVI (-)
LVI (+)
PTEN
200μm
200μm
b
PTEN
*
Immunohistochemical Score
15
10
5
0
LVI (-)
LVI (+)
c
LVI (-)
LVI (+)
p19
200μm
200μm
d
p19
*
Immunohistochemical Score
15
10
5
0
LVI (-)
LVI (+)

Figure4

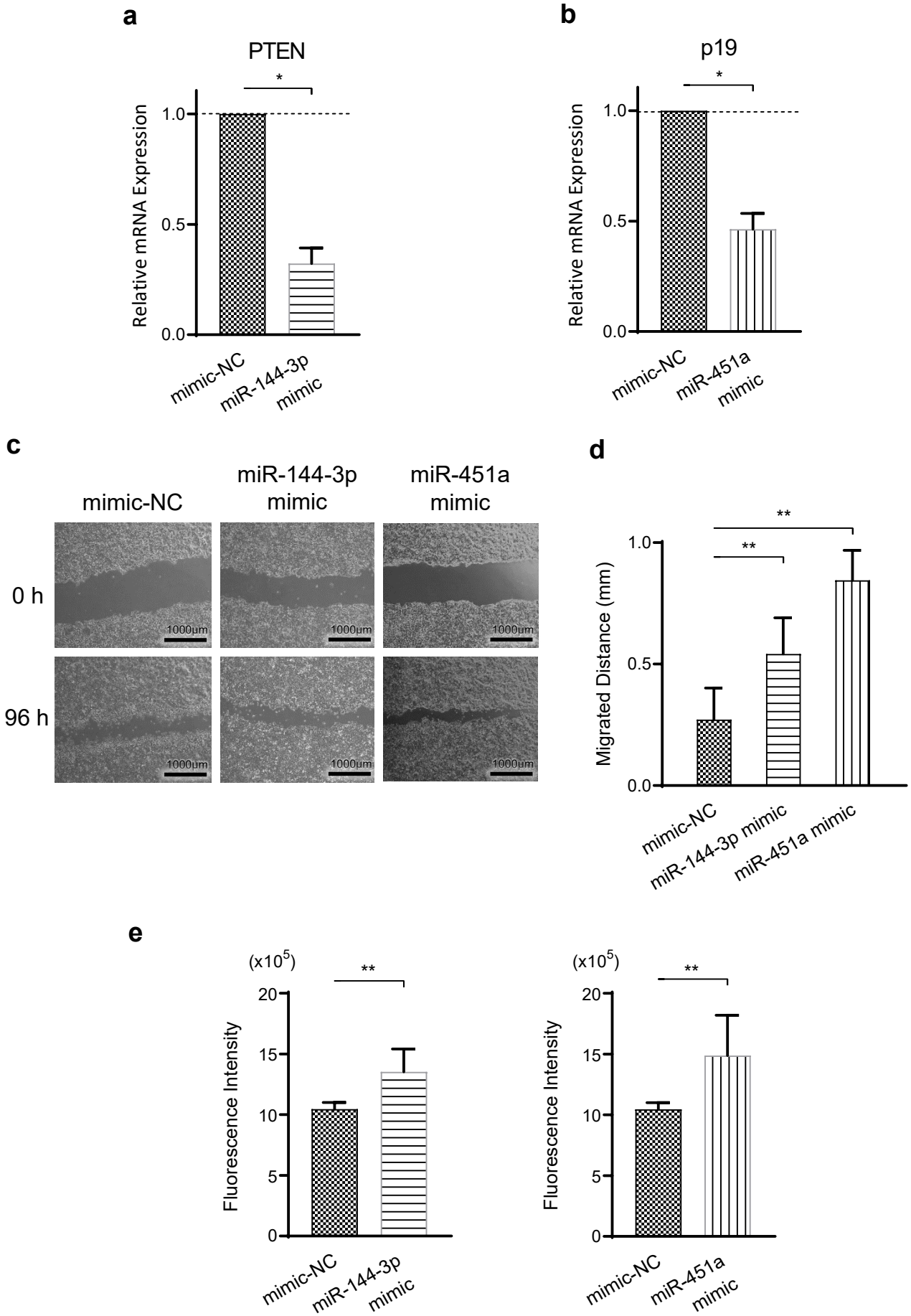
a
PTEN
*
Relative mRNA Expression
1.0
0.5
0.0
mimic-NC
miR-144-3p mimic
b
p19
*
Relative mRNA Expression
1.0
0.5
0.0
mimic-NC
miR-451a mimic
c
mimic-NC
miR-144-3p mimic
miR-451a mimic
0 h
96 h
1000μm
d
**
**
Migrated Distance (mm)
1.0
0.5
0.0
mimic-NC
miR-144-3p mimic
miR-451a mimic
e
(x10^5)
**
Fluorescence Intensity
20
15
10
5
0
mimic-NC
miR-144-3p mimic
(x10^5)
**
Fluorescence Intensity
20
15
10
5
0
mimic-NC
miR-451a mimic

Figure5

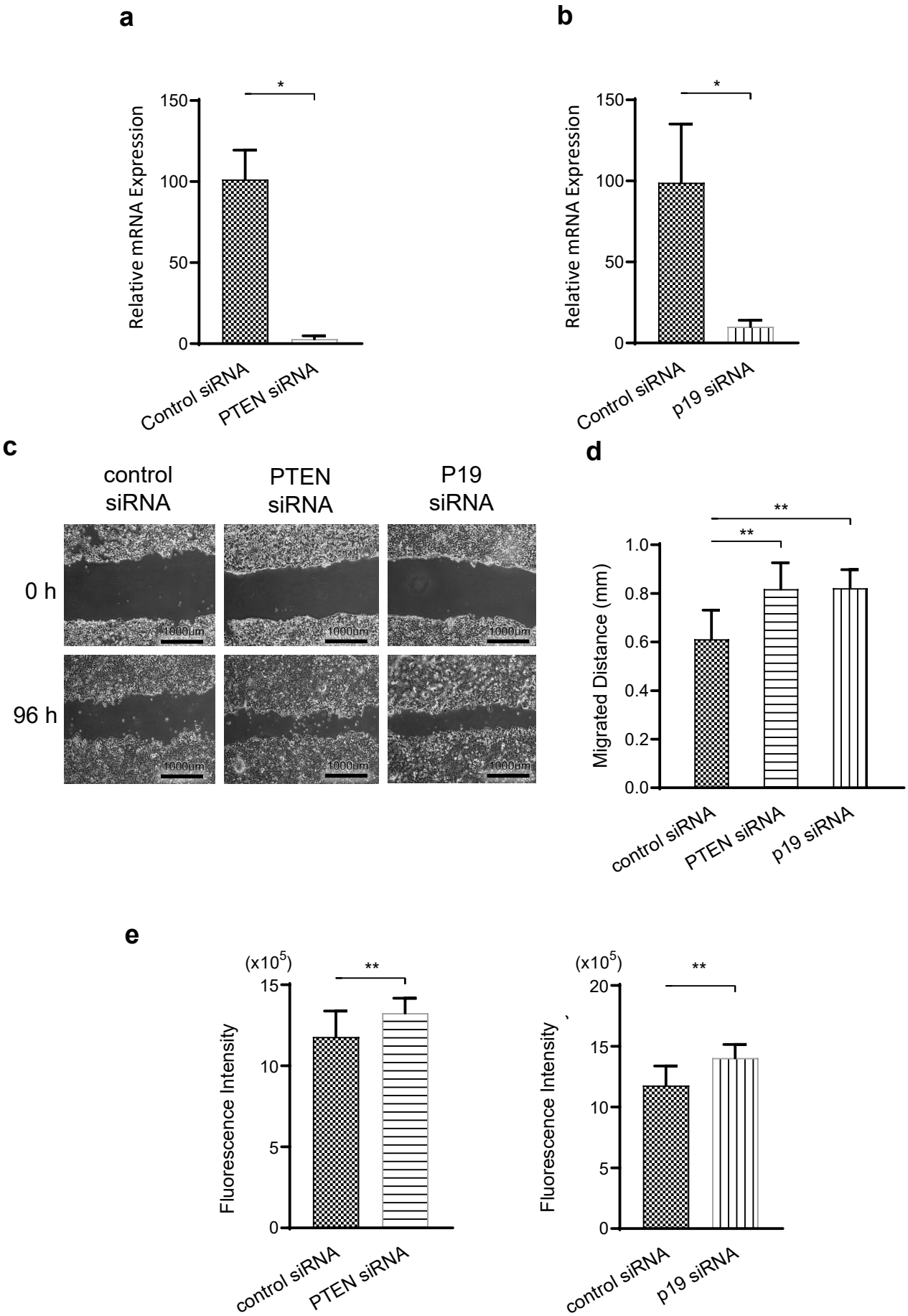
a
Relative mRNA Expression
150
100
50
0
*
Control siRNA
PTEN siRNA
b
Relative mRNA Expression
150
100
50
0
*
Control siRNA
p19 siRNA
c
control siRNA
PTEN siRNA
P19 siRNA
0 h
96 h
1000μm
d
Migrated Distance (mm)
1.0
0.8
0.6
0.4
0.2
0.0
**
**
control siRNA
PTEN siRNA
p19 siRNA
e
(x10^5)
Fluorescence Intensity
15
10
5
0
**
control siRNA
PTEN siRNA
(x10^5)
Fluorescence Intensity
20
15
10
5
0
**
control siRNA
p19 siRNA